Direct Yaw Control of Vehicle using State Dependent Riccati Equation with Integral Terms

Fargham SANDHU, Hazlina SELAMAT, Vahid Behtaji Siahkal MAHALLEH
Center for Artificial Intelligence, Universiti Teknologi Malaysia, 81310, Johor Bahru, Malaysia
hazlina@utm.my

Abstract—Direct yaw control of four-wheel vehicles using optimal controllers such as the linear quadratic regulator (LQR) and the sliding mode controller (SMC) either considers only certain parameters constant in the nonlinear equations of vehicle model or totally neglect their effects to obtain simplified models, resulting in loss of states for the system. In this paper, a modified state-dependent Ricatti equation method obtained by the simplification of the vehicle model is proposed. This method overcomes the problem of the lost states by including state integrals. The results of the proposed system are compared with the sliding mode slip controller and state-dependent Ricatti equation method using high fidelity vehicle model in the vehicle simulation software package, Carsim. Results show 38% reduction in the lateral velocity, 34% reduction in roll and 16% reduction in excessive yaw by only increasing the fuel consumption by 6.07%.

***Index Terms*—nonlinear equations, optimal control, quadratic programming, ricatti equation, sliding mode control.**

I. INTRODUCTION

Vehicles move when torque generated by the engine is transferred to the ground through the tires, generating traction forces. These forces can be measured using accelerometers alone when the vehicle is static and the kinematics equation with gyroscopes can be used when it is in motion.

When designing a controller to assist drivers to ensure stability, the vehicle model, its associated parameters and their changes become important. Most research on stability enhancement use the bicycle model to approximate the vehicle model, which simplifies the controller design, but provides only suboptimal performance improvements [1]. Earlier systems mostly consisted of classical control schemes used to control only the steering angle with given vehicle yaw and velocities [2]. In some cases, the four-wheel car model with approximate analytical Dug off and Fiala tire models were also considered to have a complete model, but were then simplified to obtain simpler models [3-4] to design the controllers. By introducing differential braking and traction as another variable for direct yaw control (DYC) the system became very efficient but its complexity in controller design increased [5]. Due to the nonlinear nature of the system, classical control schemes are not sufficient and so modern nonlinear controllers were introduced [6-7] such as fuzzy control [8-10, 28], sliding mode control (SMC) [11], SMC with variable differential transmission system and super twisting algorithm [12], optimal control of active front wheel steering and direct yaw control [13] using cost function [14], resulting in the simultaneous control of various important states. Similarly, active front wheel or rear wheel steering [7] or four-wheel steering [15] coupled with individual brake control [16] in different combinations are also used to have better control of the vehicle yaw [17].

Since the four-wheel model with analytical tire models is a complex nonlinear system, certain linearization schemes are used to simplify the controller design process [18]. Important parameter changes such as roll motion, pitching and weight distribution are sometimes neglected during the linearization process even though the four-wheel model considers the effects of all the forces and moments generated [19]. Parameter variations and state estimation problems also contribute in making the controller suboptimal, such as the cornering stiffness caused by the roll motion [20] and inaccurate noise models available.

Lateral stability is effectively attained by considering individual wheel braking and active steering control; but excessive braking can cause excessive vehicle speed reduction, more wear in the brakes and tire saturation, causing side-slips. Some studies have also considered braking, drive line and steering to control side-slips to reduce braking. Individual wheel braking to control individual side-slips is mostly used in anti-lock braking systems [21], since the steering inputs are considered as either zero or optimal for the situation. In direct yaw control, individual braking optimized for individual slips is not always suitable. Therefore, intended differences in braking are used to enhance the yaw performance by applying coordinated wheel braking [11-22], which is achieved by employing an appropriate brake pressure distribution scheme.

Chassis rolling is also responsible for wheel edge stiffness causing tire saturation; which can be compensated by adjusting the suspension using modulators [19] or by adjusting the steering angle and brake pressure. By compensating the chassis roll through steering angle compensation, suspension modulators are not required, as proposed in the work presented in this paper.

In this paper, the four-wheel car is modeled in state-dependent coefficient (SDC) form and used to design an optimal controller using state dependent Ricatti equation [16]; due to its ability to automatically adjust the brakes and steering with changes in brake pressure and sensor or actuator failure. The controller, in contrast to earlier works, will consider the state and parameters changes that have indirect but significant consequence on the system's stability and performance, e.g. brake pressure distribution dynamics, roll and weight distribution changes will be considered. To overcome the problem of state loss during linearization, an

This project is supported by Research University Grant 4J144 of Universiti Teknologi Malaysia and Ministry of Education Malaysia.

Digital Object Identifier 10.4316/AECE.2016.02014

appropriate number of integrals terms that replace lost states in the system are proposed. The extra states may increase the system dynamics but their effect on the system stability through simulations are proved to be not significant at all.

II. VEHICLE MODEL

Fig.1 shows the forces acting on the four-wheel vehicle during motion. In this figure, the vehicle is turning when a nonzero steering angle input and individually controlled brakes are applied to the wheels. Due to the turning, the front and rear wheel experience forces along the longitudinal and lateral direction of the vehicle. The longitudinal forces on the wheels are defined as the front-left, front-right, rear-left, rear-right longitudinal forces as F_{flx}, F_{frx}, F_{rlx}, F_{rrx} respectively. Similarly, the lateral wheel forces are defined as the front-left, front-right, rear-left and rear-right lateral forces as, F_{fly}, F_{fry}, F_{rly}, F_{rry} respectively. The vehicle is moving along the longitudinal axis with a velocity V_x and slipping laterally with velocity V_y. The vehicle is also turning at a yaw rate, r while it tilts along the lateral axis with a roll angle, θ and with a roll rate, p and pitches with a pitch angle, ϕ and a pitch rate, q. The vehicle suspension spring stiffness are defined by K_i and the damper stiffness are defined by C_i; which are resolved along the longitudinal direction, as K_{xi}, C_{xi}, and along the lateral direction as K_{yi} and C_{yi}. Vector $\overline{A} = [a_x, a_y\ a_z]$ represents the accelerations measured using accelerometers. Similarly, vector $\Omega=[p\ q\ r]$ represents the angular velocities of the vehicle measured perpendicular to the axis. Other symbols used in the equations are defined in Table 1.

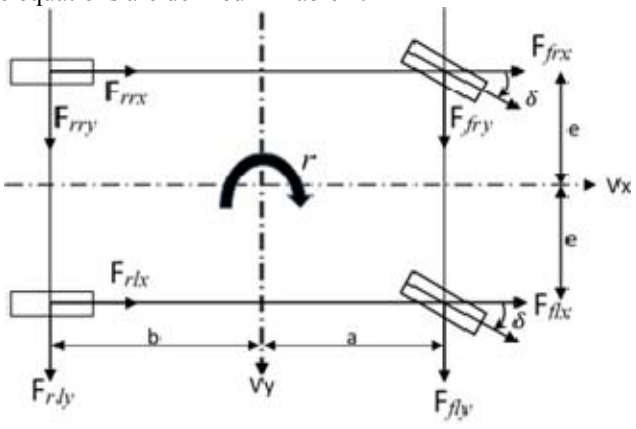

Figure 1. Force diagram of full car model

By balancing the forces along the three axis in Fig. 1, (1-8) are obtained.

$$\Sigma F = M(\mathbf{V} - \Omega_X.\mathbf{V}) = \begin{bmatrix} \Sigma F_x \\ \Sigma F_y \\ \Sigma F_z \end{bmatrix} \quad (1)$$

$$\Sigma F_x = \Sigma F_{fx}\cos\delta + \Sigma F_{rx} - \Sigma F_{fy}\sin\delta - A_p V_x |V_x| \quad (2)$$

$$\Sigma F_y = \Sigma F_{fx}\sin\delta + \Sigma F_{fy}\cos\delta + \Sigma F_{ry} - A_p V_y |V_y| \quad (3)$$

$$\Sigma F_z = Mg\cos\theta\cos\phi \quad (4)$$

$$\Sigma F_{fx} = F_{flx} + F_{frx} \quad (5)$$

$$\Sigma F_{rx} = F_{rlx} + F_{rrx} \quad (6)$$

$$\Sigma F_{fy} = F_{flx} + F_{frx} \quad (7)$$

$$\Sigma F_{ry} = F_{rly} + F_{rry} \quad (8)$$

Similarly, by balancing the moments along the roll, pitch and yaw axis, (9-14) are obtained.

$$I_z r = \Sigma M_z = \Sigma M_1 - \Sigma M_2 + \Sigma M_3 + \Sigma M_4 \quad (9)$$

$$\Sigma M_1 = a\left[\Sigma F_{fx}\sin\delta + \Sigma F_{fy}\cos\delta\right] \quad (10)$$

$$\Sigma M_2 = b\Sigma F_{ry} \quad (11)$$

$$\Sigma M_3 = e(F_{flx} - F_{frx})\cos\delta - (F_{fly} - F_{fry})\sin\delta \quad (12)$$

$$\Sigma M_4 = e\left(F_{rrx} - F_{rlx}\right) \quad (13)$$

$$I_{xx}\ddot{\phi} + m_s h_s\left[V_y - V_x r\right] = \left[m_s g h_s - K_\phi\right]\phi - C_\phi\dot{\phi} \quad (14)$$

The forces acting on the tires are obtained using (15-18).

$$F_{xi} = C_{xi}\frac{\lambda_i}{1+\lambda_i} f(\gamma_i) = J_i(\lambda_i) \quad (15)$$

$$F_{yi} = C_{yi}\frac{\tan\alpha_i}{1+\lambda_i} f(\gamma_i) = K_i\tan\alpha_i \quad (16)$$

$$\gamma_i = \frac{\mu \mathbf{F}_{zi}(1+\lambda_i)}{2\sqrt{(C_{xi}\lambda_i)^2 + (C_{yi}\tan\alpha_i)^2}} \quad (17)$$

$$f(\gamma_i) = \begin{cases} 1, & \text{if}\ \gamma_i \geq 1 \\ (2-\gamma_i)\gamma_i, & \text{otherwise} \end{cases} \quad (18)$$

Substituting (15-18) into (1-14) and simplifying as shown in Appendix A.

$$\dot{V}_x = \left[a_{11}\ a_{12}\ a_{13}\ a_{14}\ a_{15}\ a_{16}\ a_{17}\ a_{18}\right][x] + U_1 \quad (19)$$

$$\dot{V}_y = \left[a_{21}\ a_{22}\ a_{23}\ a_{24}\ a_{25}\ a_{26}\ a_{27}\ a_{28}\right][x] + U_2 \quad (20)$$

$$U_1 = b_{11}\dot{\phi} + b_{12}\phi,\ U_2 = b_{21}\dot{\phi} + b_{22}\phi \quad (21)$$

$$M_1 = M + \frac{m_s^2 h_s^2}{I_{xx}} \quad (22)$$

$$\dot{r} = \left[a_{31}\ a_{32}\ a_{33}\ a_{34}\ a_{35}\ a_{36}\ a_{37}\ a_{38}\right][x] \quad (23)$$

Here, a_{ij}'s are the coefficients of the state matrix as defined in appendix A. In [11, 16, 17, 23], $\dot{\phi} \approx 0$ and $\phi \approx 0$ were considered for simplicity, implying that $M_1 \approx M$ and so the weight distribution effects on the lateral velocity were not considered. In the proposed system, their effect is compensated by introducing extra states through integral action. The indirect effect of these parameters e.g. the roll effect on weight distribution and lateral velocity as described by (14), is calculated using the roll model [3], given by (24).

$$\ddot{\phi} = -\frac{C_\phi}{I_{xx}}\dot{\phi} - \frac{(K_\phi - m_s g h_s)}{I_{xx}}\phi + \frac{m_s h_s}{I_{xx}}a_y \quad (24)$$

Similarly, the slip across each tire is modeled using the vehicle traction model [16]. The vehicle slip is modeled in (24), in terms of input tire torque, T_{bi} generated by the

brake pressure, engine and transmission dynamics and modeled as a nonlinear component; creating more states which justifies the addition of new states as integral terms. The variable is calculated for each wheel.

$$\dot{\lambda}_i = -\frac{R_i^2 J_i \lambda_i}{I_w V_x} - (\lambda_i + 1)\frac{\dot{V}_x}{V_x} - \frac{R_i T_{bi}}{I_w V_x} \tag{25}$$

By substituting (19) into (24), the dynamic slip rate is calculated in (25). The coefficients of which are listed in Appendix A.

$$\dot{\lambda}_i = \begin{bmatrix} a_{i1} & a_{i2} & a_{i3} & a_{i4} & a_{i5} & a_{i6} & a_{i7} & a_{i8} \end{bmatrix} [x] + b_{i1}\dot{\phi} + b_{i2}\phi \tag{26}$$

Similarly, the system steering input is augmented by the steering actuator, modeled as a first order delay system [16].

$$\dot{\tilde{\delta}} = \begin{bmatrix} a_{41} & a_{42} & a_{43} & a_{44} & a_{45} & a_{46} & a_{47} & a_{48} \end{bmatrix} [x] + b_{44}\delta_c \tag{27}$$

In the model, the roll is estimated from a two-state estimator obtained from (14) and listed in (27). [31]

$$\begin{bmatrix} \ddot{\phi} \\ \dot{\phi} \end{bmatrix} = \begin{bmatrix} -\frac{C_\phi}{I_{xx}} & -\frac{K - m_s g h_s}{I_{xx}} \\ 1 & 0 \end{bmatrix} \begin{bmatrix} \dot{\phi} \\ \phi \end{bmatrix} + \begin{bmatrix} \frac{mh}{I_{xx}} \\ 0 \end{bmatrix} a_y \tag{28}$$

Where

$$a_y = \mathrm{V_y} + r V_x \tag{29}$$

The roll model states $\begin{bmatrix} \hat{\dot{\phi}} \\ \hat{\phi} \end{bmatrix}$ are used to calculate the roll stiffness forces in the four wheels, using (30).

$$\begin{bmatrix} F_{\phi 1} \\ F_{\phi 2} \\ F_{\phi 3} \\ F_{\phi 4} \end{bmatrix} = \begin{bmatrix} C_{\phi f} & K_{\phi f} \\ C_{\phi f} & K_{\phi f} \\ C_{\phi r} & K_{\phi r} \\ C_{\phi r} & K_{\phi r} \end{bmatrix} \begin{bmatrix} \dot{\phi} \\ \phi \end{bmatrix} \tag{30}$$

The effects of roll on the weight distribution are included in the tire reaction forces of each wheel, using (27-30) [16].

$$F_z = \begin{bmatrix} \frac{m_s g b}{2l} - \frac{m_s h_s}{2l}\dot{V}_x - \frac{bmh}{2el}\dot{V}_y - F_{\phi 1} \\ \frac{m_s g b}{2l} - \frac{m_s h_s}{2l}\dot{V}_x + \frac{bmh}{2el}\dot{V}_y + F_{\phi 2} \\ \frac{m_s g a}{2l} + \frac{m_s h_s}{2l}\dot{V}_x - \frac{bmh}{2el}\dot{V}_y + F_{\phi 3} \\ \frac{m_s g a}{2l} + \frac{m_s h_s}{2l}\dot{V}_x + \frac{bmh}{2el}\dot{V}_y - F_{\phi 4} \end{bmatrix} \tag{31}$$

In a state-dependent coefficient (SDC) form, the nonlinear vehicle dynamic in (19-23, 26, 27) are rewritten in a linear state space representation form as given by (32-33).

$$\dot{x} = A(x)x + B(x)u \tag{32}$$

$$y = Cx + Du \tag{33}$$

Whereas the u matrix consists of the inputs, listed in (34)

$$u = \begin{bmatrix} \hat{\dot{\phi}} & \hat{\phi} & \tilde{\delta} & T_{b1} & T_{b2} & T_{b3} & T_{b4} \end{bmatrix} \tag{34}$$

The coefficients of state matrix A(x) and input matrix B(x) as described in (33) and (34) are listed in (61-92) of Appendix-A, in terms of the state vector x= [

$x_1\ x_2\ x_3\ x_4\ x_5\ x_6\ x_7\ x_8\ ] = [\ V_x\ V_y\ r\ \delta\ \lambda_1\ \lambda_2\ \lambda_3\ \lambda_4\ ]$.

The state matrix is coefficients are defined in (62-93). Similarly, the B(x) matrix consists of various state dependent coefficients, listed in (94-99) in Appendix-A

$$A(x) = \begin{bmatrix} a_{11} & a_{12} & a_{13} & a_{14} & a_{15} & a_{16} & a_{17} & a_{18} \\ a_{21} & a_{22} & a_{23} & a_{24} & a_{25} & a_{26} & a_{27} & a_{28} \\ a_{31} & a_{32} & a_{33} & a_{34} & a_{35} & a_{36} & a_{37} & a_{38} \\ a_{41} & a_{42} & a_{43} & a_{44} & a_{45} & a_{46} & a_{47} & a_{48} \\ a_{51} & a_{52} & a_{53} & a_{54} & a_{55} & a_{56} & a_{57} & a_{58} \\ a_{61} & a_{62} & a_{63} & a_{64} & a_{65} & a_{66} & a_{67} & a_{68} \\ a_{71} & a_{72} & a_{73} & a_{74} & a_{75} & a_{76} & a_{77} & a_{78} \\ a_{81} & a_{82} & a_{83} & a_{84} & a_{85} & a_{86} & a_{87} & a_{88} \end{bmatrix} \tag{35}$$

The B(x) matrix is modified to include the estimated roll and roll rate obtained from (28).

$$B(x) = \begin{bmatrix} 0 & b_{12} & 0 & 0 & 0 & 0 & 0 \\ b_{21} & 0 & 0 & 0 & 0 & 0 & 0 \\ 0 & 0 & b_{44} & 0 & 0 & 0 & 0 \\ 0 & b_{52} & 0 & b_{55} & 0 & 0 & 0 \\ 0 & b_{62} & 0 & 0 & b_{66} & 0 & 0 \\ 0 & b_{72} & 0 & 0 & 0 & b_{77} & 0 \\ 0 & b_{82} & 0 & 0 & 0 & 0 & b_{88} \end{bmatrix} \tag{36}$$

While C and D are constants.

$$C = \begin{bmatrix} 0&0&0&1&0&0&0&0 \\ 0&0&0&0&1&0&0&0 \\ 0&0&0&0&0&1&0&0 \\ 0&0&0&0&0&0&1&0 \\ 0&0&0&0&0&0&0&1 \end{bmatrix},\ D = \begin{bmatrix} 0&0&0&0&0&0&0&0 \\ 0&0&0&0&0&0&0&0 \\ 0&0&0&0&0&0&0&0 \\ 0&0&0&0&0&0&0&0 \\ 0&0&0&0&0&0&0&0 \\ 0&0&0&0&0&0&0&0 \\ 0&0&0&0&0&0&0&0 \\ 0&0&0&0&0&0&0&0 \end{bmatrix} \tag{37}$$

III. REFERENCE SLIP ESTIMATION

During equilibrium, the net force acting on the vehicle is $F \approx [0\ 0\ g]^T$; which is defined according to (1) in (38).

$$\dot{V} = A = [0\ 0\ g]^T = \Omega_X V + N \tag{38}$$

$$\Omega_X = \begin{bmatrix} 0 & -r & q \\ r & 0 & -p \\ -q & p & 0 \end{bmatrix} \tag{39}$$

The function Ω_X has special properties, it is skew symmetric $(\Omega_X{}^T = -\Omega_X)$ and so it satisfies Lie algebra. The matrix does not have any inverse. The relevant states for longitudinal and lateral stability are obtained using (40).

$$y = \begin{bmatrix} \dot{V}_x \\ \dot{V}_y \end{bmatrix} = \begin{bmatrix} 1&0&0 \\ 0&1&0 \end{bmatrix} \begin{bmatrix} \dot{V}_x \\ \dot{V}_y \\ \dot{V}_z \end{bmatrix} \tag{40}$$

The states obtained in y are important for estimating the reference slip in terms of the longitudinal and lateral accele rations and measured yaw rate, which can be obtained from the instantaneous velocities changes and measured yaw rate using (41). It is also assumed that the acceleration due to gravity is constant and there is only vertical motion of the tires and no sideways motion is caused due to misalignments of the camber and kingpin angles. The camber angle may cause negligible motion of the wheels sideways due to the rubber bushings in the suspension.

In (38), N is the error that increases during turning or braking. It is assumed that the error is negligible during driving in a straight line.

$$\lambda_d = 100\tan^{-1}\left(\frac{\dot{V}_y}{\dot{V}_x}\right)+100r = 100\tan^{-1}\left(\frac{a_y}{a_x}\right)+100r \quad (41)$$

IV. CONTROLLER DESIGN

The vehicle SDC form given in (32) is used in designing the controller. The state equation along with the integral terms is presented by the equation in (42).

$$\dot{\mathbf{z}} = \begin{bmatrix} A(x) & O \\ -C & O \end{bmatrix}\mathbf{z} + \begin{bmatrix} B(x) \\ O \end{bmatrix}u = \Gamma(z)z + \Theta(z)u \quad (42)$$

Where

$$\mathbf{z} = \begin{bmatrix} x \\ w_1 \end{bmatrix},\ w_1 = \int_{t_0}^{\infty} x dx = C\int_{t_0}^{\infty} x\,dt \quad (43)$$

With the inputs consisting of the feedback gain and state error terms (43)

$$u = R^{-1}\Theta(z)^T P(z)\begin{bmatrix} \tilde{x} \\ \tilde{x}_1 \end{bmatrix} \quad (44)$$

Where P (z) is the co-variance matrix obtained by solving the Ricatti equation given in (45) starting with the initial conditions.

$$P(z)\Gamma(z) + \Gamma(z)^T P(z) + P(z)\Theta(z)K + \begin{bmatrix} Q_i & 0 \\ 0 & Q_j \end{bmatrix} = 0 \quad (45)$$

Where

$$K = R^{-1}\Theta(z)^T P(z) \quad (46)$$

In this equation R, Q_i and Q_j are constants obtained by optimizing the cost function for optimal performance. The matrices Q_i, Q_j and R are given in (54-56). The input matrix B(x) = g(x) and state matrix A(x) are considered to be observable and detectable for each value of x.

By assuming the inputs to the system are bounded and smooth near the vicinity of zero, the system is considered to be controllable and observable in a region Ω, defined by the stable and observable states, provided it is point wise observable and detectable for all states x [16]. The controllability region Ω is defined by the states that satisfy the conditions and the controllability and observability conditions as follows:

$$\text{Rank [A, AB...]} = \text{Rank [A]} \quad (47)$$

$$\text{Rank [O]} = \text{Rank [A, AC...]} = \text{Rank [A]} \quad (48)$$

The controllability region of the system without integral terms has already been defined in [16], which is also true for the proposed system.

In (49), the integrals of the individual slips and the steering inputs are included and the remaining three integrals of longitudinal velocity V_x, lateral velocity V_y and yaw rate r are not included since their integrals have no effect on the system performance. The feedback gains are obtained from the Ricatti equation solution (46). According to Lyapunov theory, the cost function must include the system states and inputs to optimize the state variables as given in (49).

$$J = \int_{t_0}^{\infty} [\tilde{x}^T Q_i \tilde{x} + u^T R_1 u + x_1^T Q_j w_1]dx \quad (49)$$

Where the state error vector is written in (50)

$$\tilde{x} = x - x_{ref} \quad (50)$$

And the integral terms are updated by the integration of the current state and reference state difference in (51)

$$\tilde{x}_1 = \int_{t_0}^{\infty} [\delta_d - \delta, \lambda_d - \lambda_1, \lambda_d - \lambda_2, \lambda_d - \lambda_3, \lambda_d - \lambda_4]^T dx \quad (51)$$

Where x_{ref} is given in (52)

$$x_{ref} = [V_{xref}, 0, 0, \delta_d, \lambda_d, \lambda_d, \lambda_d]^T \quad (52)$$

$$V_{xref} = V_{x0} \quad (53)$$

$$Q_i = \begin{bmatrix} 1 & 0 & 0 & 0 & 0 & 0 & 0 & 0 \\ 0 & 100 & 0 & 0 & 0 & 0 & 0 & 0 \\ 0 & 0 & 100 & 0 & 0 & 0 & 0 & 0 \\ 0 & 0 & 0 & 0.2 & 0 & 0 & 0 & 0 \\ 0 & 0 & 0 & 0 & 100 & 0 & 0 & 0 \\ 0 & 0 & 0 & 0 & 0 & 100 & 0 & 0 \\ 0 & 0 & 0 & 0 & 0 & 0 & 100 & 0 \\ 0 & 0 & 0 & 0 & 0 & 0 & 0 & 100 \end{bmatrix} \quad (54)$$

$$Q_j = \begin{bmatrix} 0.2 & 0 & 0 & 0 & 0 \\ 0 & 50 & 0 & 0 & 0 \\ 0 & 0 & 50 & 0 & 0 \\ 0 & 0 & 0 & 50 & 0 \\ 0 & 0 & 0 & 0 & 50 \end{bmatrix} \quad (55)$$

$$R_1 = \begin{bmatrix} 1 & 0 & 0 & 0 & 0 & 0 & 0 \\ 0 & 1 & 0 & 0 & 0 & 0 & 0 \\ 0 & 0 & 1 & 0 & 0 & 0 & 0 \\ 0 & 0 & 0 & 10^{-4} & 0 & 0 & 0 \\ 0 & 0 & 0 & 0 & 10^{-4} & 0 & 0 \\ 0 & 0 & 0 & 0 & 0 & 10^{-3} & 0 \\ 0 & 0 & 0 & 0 & 0 & 0 & 10^{-3} \end{bmatrix} \quad (56)$$

The cost function (49) is an important parameter since it represents the overall performance of the system. The proposed cost function includes the integral terms to consider second order dynamics. The effect of the integral terms to system response is similar to the effect of the integral terms in PI controllers for second order linear systems.

Similar cost function, without integral terms, is used in the implementation of state dependent riccati equation as given in (57) [16]. This cost function will be used in the performance analysis of SDRE and SM-slip control.

$$J = \int_{t_0}^{\infty} [\tilde{x}^T Q_i \tilde{x} + u^T Ru]dx \quad (57)$$

Where

$$R = \begin{bmatrix} 1 & 0 & 0 & 0 & 0 \\ 0 & 10^{-4} & 0 & 0 & 0 \\ 0 & 0 & 10^{-4} & 0 & 0 \\ 0 & 0 & 0 & 10^{-3} & 0 \\ 0 & 0 & 0 & 0 & 10^{-3} \end{bmatrix} \quad (58)$$

The stability of the system using the cost function (57) has already been satisfied in [16]. Since the proposed cost function is similar to the state dependent riccati equation cost function, the proposed cost function is also proved to represent a stable system in the same manner.

Using the following theorem, the system is proved to represent a stable system at every point of the state matrix x.

Theorem 1. During the linearization of f(x) = A(x), g(x) = B(x), if the resultant matrices are smooth, detectable and

controllable, then SDRE method generates a closed loop solution, which is locally and asymptotically stable [16].

Proof: The closed loop system is defined as follows:

$$\dot{z}=\begin{bmatrix}(A(x)-B(x)R^{-1}B(x)^{T}P(x))x\\-Cz\end{bmatrix}=\Gamma_{c}z=\begin{bmatrix}A_{c}\\-C\end{bmatrix}z \quad (59)$$

The closed loop matrix Γ_c has already been proved to be stable at all points of z according to the Riccati equation theory [16, 24, 27]. The other term simply defines the relationship of the integral terms. If A(x) is smooth and bounded, then the system is detectable and stable and becomes zero at the neighborhood of x = [0], the neighborhood of boundedness can be found using Taylor series expansion [16].

The optimality condition for state dependent riccati equation is already proved for a scaler system [28]. The necessary condition for optimality $\dot{P}(x)x+\dot{x}P(x)+H_{x}=0$ is not generally proved for the SDRE, and is asymptotically satisfied only in the quadratic rate sense and produces suboptimal results [16]. H_z is the Hamilton of state matrix calculated in terms of z. By comparing the stability condition with (45)

$$H_{z}=P(z)\Theta(z)K+\begin{bmatrix}Q_{i} & 0\\0 & Q_{j}\end{bmatrix}\approx 0, For\ K=R^{-1}\Theta(z)^{T}P(z) \quad (60)$$

According to (60), if a Ricatti solution of P(z) exists, the solution is guaranteed to be optimal.

The proposed system optimality condition $\dot{P}(z)z+\dot{z}P(z)+H_{z}=0$ is also not generally satisfied, and is optimally satisfied in the quadratic rate sense in the same manner since the only difference between the proposed system and SDRE is the inclusion of the integral terms which add extra poles at s=0 [27].

Since the system stability depends upon the system inputs, which must be smooth and bounded [16, 24]. In real systems, the steering input is applied through actuators, which causes smooth turning to the vehicle and is limited by the steering column and actuator limits. In the proposed method, the following limits are applied to the steering angle input [24].

$$\delta=\begin{cases}\dfrac{-\pi}{16} & if\ \ \tilde{\delta}\le\dfrac{-\pi}{16}\\[2mm]\dfrac{\pi}{16}\sin\tilde{\delta} & if\ \ \dfrac{-\pi}{16}\le\tilde{\delta}\le\dfrac{\pi}{16}\\[2mm]\dfrac{\pi}{16} & if\ \ \tilde{\delta}\ge\dfrac{\pi}{16}\end{cases} \quad (61)$$

V. SIMULATION OF THE PROPOSED SYSTEM

The system is simulated using Matlab Simulink and Carsim simulator. The simulator is programmed with the actual vehicle parameters given in Table.1.

TABLE 1: IMPORTANT PARAMETERS USED DURING SIMULATION

Symbol	Definition	Value
a	Distance of front wheel from center of gravity (c.g)	0.820 m
b	Distance of rear wheel from c. g	1.620 m
l	Distance between front wheel and rear wheels	2.440 m
w	Wheel base	1.455 m
e	Distance between front tires	1.460 m
t	Tread width	0.81 m
h_s	Height of c.g from ground	0.6 m
M	Total mass of vehicle	1528.2 Kg
m_s	Sprung mass of vehicle	1200 Kg
I_z	Moment of inertia along z-axis	2400 Kgm^2
I_{xx}	Moment of inertia along x-axis	1100 Kgm^2
m_t	Mass of tire	30 Kg
I_w	Moment of inertia of tire	2750 Kg^2
r_t	Radius of tire	0.29155m
K_t	Spring constant of tires	$1.9\,e^{5}\,Nm^{-1}$
C_{xf}	Coefficient of front tires along x-axis	916 Ns/rad
C_{yf}	Coefficient of front tires along y-axis	916 Ns/rad
C_{xr}	Coefficient of rear tires along x-axis	152788 Ns/rad
C_{yr}	Coefficient of rear tires along y-axis	152788 Ns/rad
$K_{\phi f}$	Roll stiffness of front tires	25200 N/m
$C_{\phi f}$	Roll damping of front tires	105 Ns/rad
$K_{\phi r}$	Roll stiffness of rear tires	25200 N/m
$C_{\phi r}$	Roll damping of rear tires	105 Ns/rad

Stability of vehicles is most crucial during heavy braking or fast accelerating, steep turning, and during overcoming uneven and varying friction surfaces. Therefore, the split-μ test and the high speed lane change tests are used in the evaluation of the proposed controller. These tests are the default tests used to test turn over problem and are mandatory for vehicles.

The system tests disturbances are input to the controller as well as the Carsim software. The vehicle chosen is class B utility vehicle without ABS, to ensure ABS system does not effect the results. The vehicle transmission consists of independent Macpherson front suspension and twisted beam rear suspension according to the actual vehicle. The vehicle roll dynamics are obtained from Carsim software for plotting. The proposed test system block diagram is given in Fig.3.

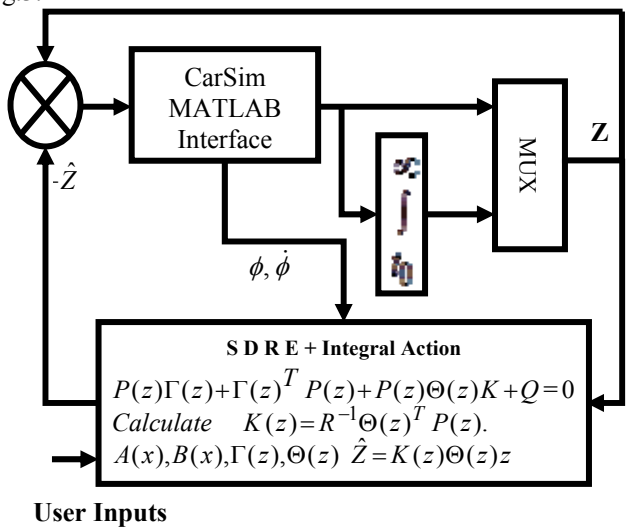

Figure 3. Block diagram of the system

The system is tested with a suitable sample time Ts = 0.01

[29]. The state matrix A(x), B(x), $\Gamma(z)$, $\Theta(z)$ are obtained using Appendix A and (37). The state matrices are calculated at each sample point and used in the same sample interval for calculations.

A. Split-μ Test

In this test, the vehicle is running at high speed (72Km/h) on a straight road without driver input (δ=0), and the road surface was switched from a high friction (μ=0.8) to low friction (μ=0.50) after 2s as shown in Fig. 2.

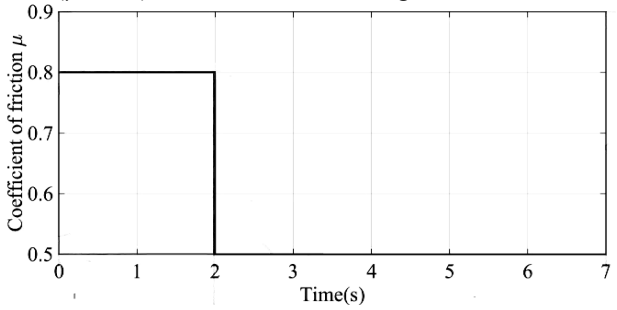

Figure 2. Friction Coefficient applied to the left side wheels of the vehicle

B. High Speed Lane Change Test

In the second test, the vehicle was turning at a high yaw rate to illustrate the performance of the controller in assisting the driver during a high-speed lane change. The drop in velocity during the turn was due to the intervention of the brakes in order to reduce the speed of the vehicle, making it suitable for taking the turn. A large angle steering input is applied to the vehicle, which is traveling at a speed of 72Km/h as shown in Fig. 3. The road surface friction is μ = 0.8.

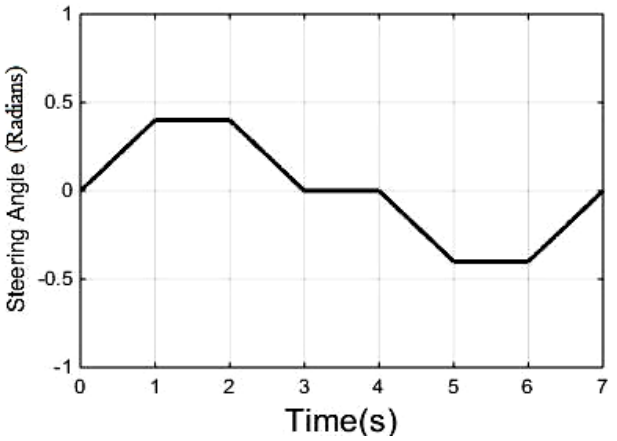

Figure 3. Steering Input to the system during high-speed lane change test.

VI. RESULTS AND ANALYSIS

A. Split-μ Test

The split-μ test is performed to illustrate how the extra states in the proposed controllers (SDRE with integral terms) have affected the system dynamics as compared to the existing state dependent Ricatti (SDRE) and sliding mode slip controllers (SM-slip). In this test the change in lateral velocity and yaw rate is increased by the proposed controller because extra states tend to increase the system dynamic response as shown in Figs. 4 and 6.

However, this increase does not considerably affect the system performance since the changes in the lateral velocity and yaw rate are still negligible. This implies, the weight imbalances are not significant because the external centripetal forces produced by the slip are negligible, as shown in Fig. 5. The negligible effect of the external centripetal forces is due to the ability of the controllers to overcome the tire saturation region during the test and results in a very small slip values across each tire as shown in Fig. 8.

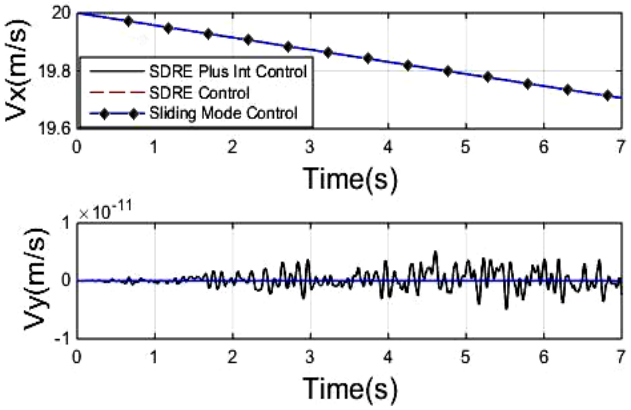

Figure 4. Horizontal Velocity V_x and Lateral Velocity V_y in split-μ test

The changes in each parameter during the test are listed in Table 2. The cost function for SDRE is calculated using (57), while the cost function for the proposed system is calculated using (49). The cost function used for SM-slip control is also (56) because the states used in its design are similar to the states used in SDRE and according to Lyapunov theory for nonlinear systems, the cost function must include the relevant state and input control signal energies only.

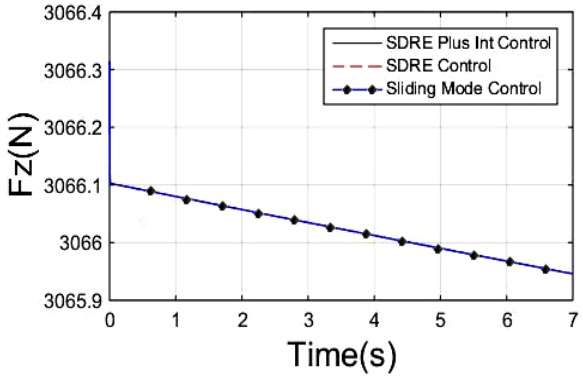

Figure 5. Changes in Vertical Force F_z during Split-μ Test.

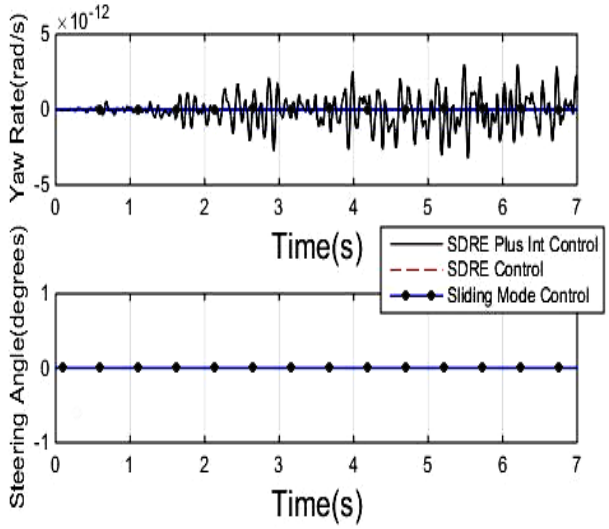

Figure 6. Yaw rate of the vehicle during split-μ test.

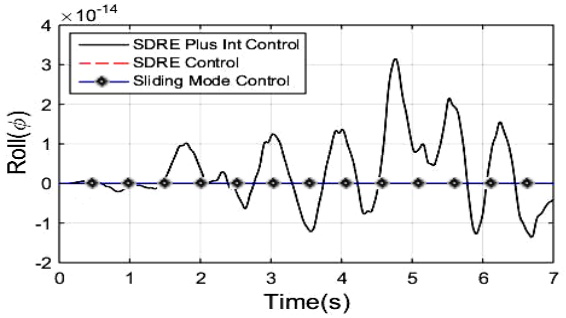

Figure 7. Roll angle during split-μ Test.

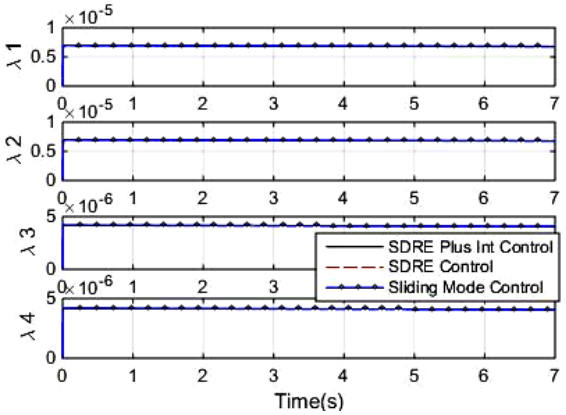

Figure 8. Slip across the front left wheel during Split-μ Test.

TABLE 2. IMPORTANT PARAMETERS DURING SPLIT-μ TEST

Parameter	SDRE with Integral action	SDRE	SM-slip
V_y (m/s)	$5.13\,e^{-12}$	$2.17\,e^{-16}$	$1.87\,e^{-17}$
V_x (m/s)	19.71	19.71	19.68
Yaw rate (r) (degree/s)	$3.03\,e^{-12}$	$1.33\,e^{-16}$	$6.16\,e^{-18}$
Cost function, J	400	400	440

B. High Speed Lane Change Test

The purpose of this test is to show effectiveness of the proposed controller compared to the state dependent Ricatti (SDRE) controller and sliding mode slip controllers (SM-Slip). In this test, lower lateral velocities and yaw rates indicate better vehicle performance as the vehicle is drifting less when commanded, by overcoming tire saturation. In this test, the proposed controller has reduced the lateral velocity by 38% compared to the SDRE controller and 29% compared to the SM-Slip controller as shown in Fig. 9.

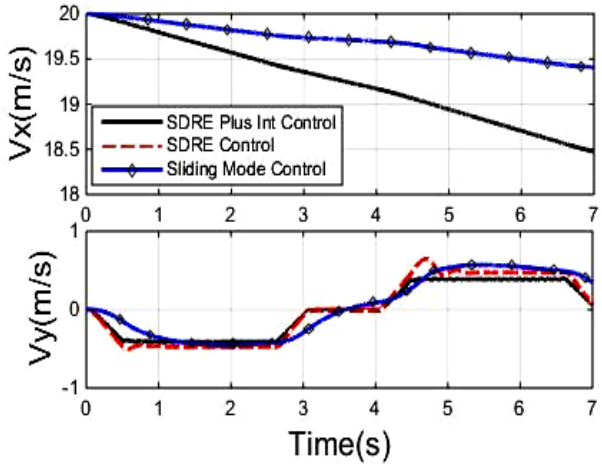

Figure 9. The Horizontal Velocity V_x and Lateral Velocity V_y during lane change test.

In Fig. 9 higher reduction in longitudinal velocities indicate that the vehicle is applying more braking forces to achieve stability, which will result in higher fuel consumption. So the proposed controller has increased the fuel consumption by 6.07% as compared to the referenced controllers as shown in Fig. 9, which is a drawback of the proposed controller.

Similarly, excessive yaw rate is reduced by 16% as compared to the SDRE controller and 2.8% as compared to the SM-Slip controller, as shown in Fig. 10. The integral terms have reduced the yaw rate overshoot, similar to the effect of integral terms in PI control for second order linear systems. Similar reduction in the steady state error can be anticipated. In the s-domain, the integral terms can be considered as creating extra poles at s = 0 [7].

The sliding mode slip control is loosely following the same yaw rate with respect to steering input. This indicates the controller has less control on the yaw rate.

Since the roll induced in the chassis during motion is primarily due to the force imbalances caused by the uncompensated centripetal forces, which must be minimized. The proposed controller has 7.6% less vertical force changes as compared to SDRE and sliding mode slip controller as shown in Fig. 11.

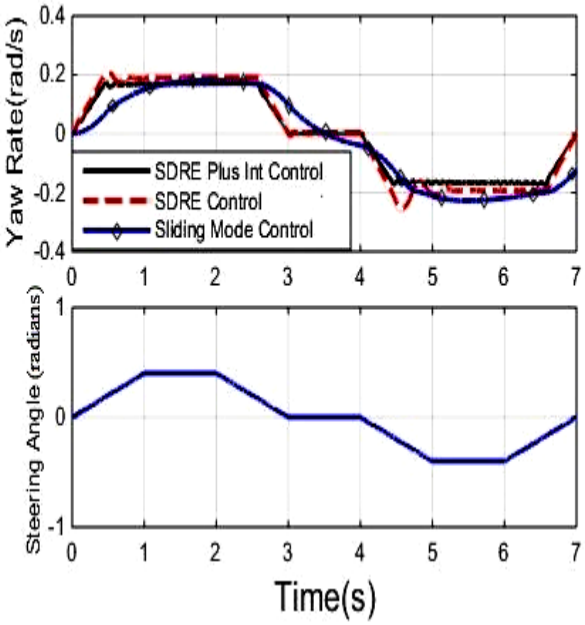

Figure 10. Yaw rate of the vehicle during lane change test.

Similarly, the roll angle is also a by-product of the force imbalances of the vehicle along the lateral direction. The proposed controller reduces the roll angle by 34% as compared to the referenced controllers as shown in Fig. 12.

The roll angle changes during the tests are very small but their effect on the weight distributions is significant, so they are not neglected. The overall improvements in the system performance can be measured in terms of the reduction in slips, which are also reduced as shown in Fig. 13.

Table.3 below lists the important parameters measured during the test. The values of cost function J are calculated using (49) for the proposed system and (57) for SDRE and SM-slip controllers; which satisfies the cost function requirements as defined by Lyapunov function for non-linear control systems.

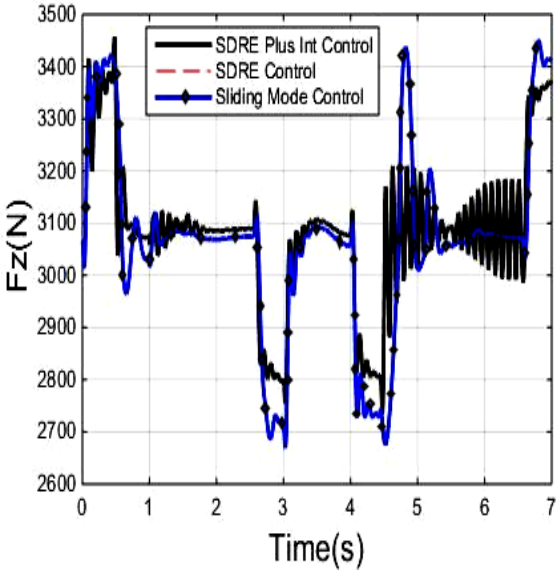

Figure 11. F_z Changes during lane change test.

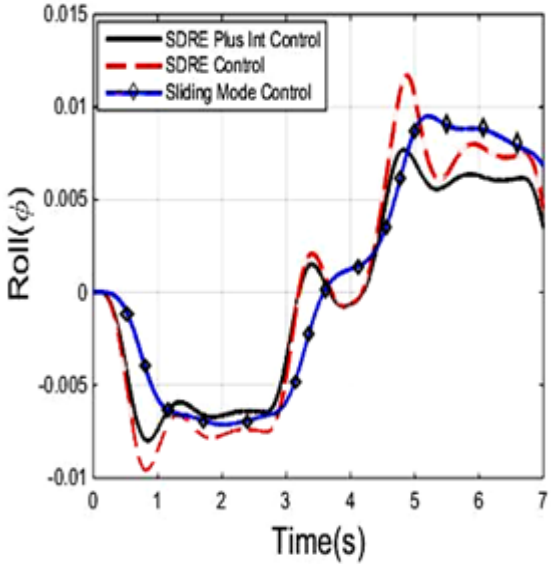

Figure 12. Chassis roll angle change during lane change test.

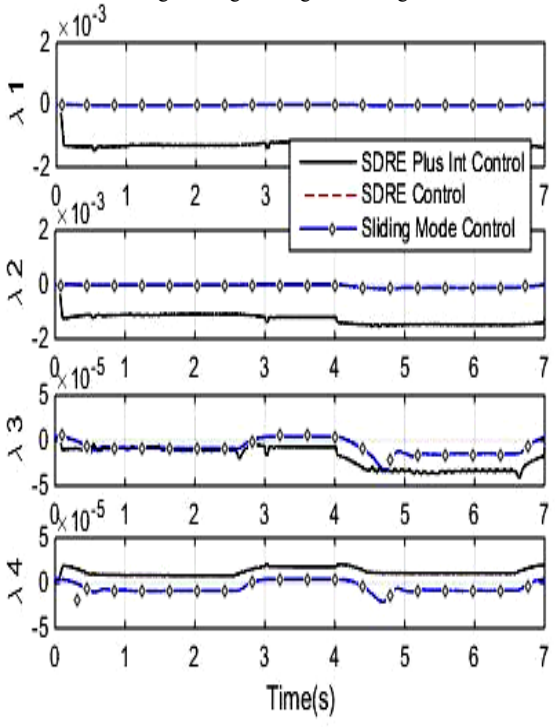

Figure 13. Slip across the front left wheel during lane change test.

TABLE 3. IMPORTANT PARAMETERS DURING LANE CHANGE TEST

Parameter	SDRE with integral action	SDRE	SM-slip
V_y (m/s)	0.400	0.650	0.571
V_x (m/s)	18.454	19.408	19.230
ΔF_z (N)	720.477	780.4	790.9
Max. Roll (radians)	0.008	0.012	0.010
Yaw rate (r) (radians/s)	0.174	0.209	0.179
Cost Function, J	415.085	432.41	480.560

VII. CONCLUSION

The paper proposes a new controller that includes the states that are normally neglected in many controller design approaches. These parameters, despite having minimal effects on the system outcome, are important for improving the vehicle stability at higher speeds. The proposed controller uses the state dependent riccati equation (SDRE) controller with integral terms; which is tested against the controller based on the SDRE and sliding mode slip controller. The proposed controller shows reduction in lateral velocity and yaw rate as well as reduction in chassis roll at the expense of 6.07% more speed reduction as compared to SDRE and sliding mode based slip controller in the double lane change test. This is a drawback of the proposed controllers. However, by adjusting the cost function, the drop in the velocity can be reduced further, improving the fuel efficiency. The proposed controller did not include changes in the tire coefficients due to temperature effects and ageing. Similarly, better tire models can be used to improve the system.

APPENDIX A

After simplifying (2-14) using tire equations (15-18), the state matrix and input matrix coefficient terms as used in (19-26) in terms of states are defined in (62-93)

$$a_{11}=-\frac{A_p|x_1|}{M_1} \tag{62}$$

$$a_{12}=\left[\frac{K_1\sin x_4}{M_1(x_1+ex_3)}+\frac{K_2\sin x_4}{M_1(x_1-ex_3)}+x_3\right] \tag{63}$$

$$a_{13}=-\left[\frac{K_1 a\sin x_4}{M_1(x_1+ex_3)}+\frac{K_2 a\sin x_4}{M_1(x_1-ex_3)}\right] \tag{64}$$

$$a_{14}=\frac{K_1\sin x_4+K_2\sin x_4}{M_1} \tag{65}$$

$$a_{15}=\frac{J_1\cos x_4}{M_1},a_{16}=\frac{J_2\cos x_4}{M_1} \tag{66}$$

$$a_{17}=\frac{J_3}{M_1},a_{18}=\frac{J_4}{M_1} \tag{67}$$

$$a_{21}=\frac{(M+m_s{}^2h_s{}^2)x_4}{M_1} \tag{68}$$

$$a_{22}=\left[\frac{K_1\cos x_4+K_4}{M_1(x_1+ex_3)}+\frac{K_2\cos x_4+K_3}{M_1(x_1-ex_3)}+\frac{A_p|x_2|}{M_1}\right] \tag{69}$$

$$a_{23}=\left[\frac{K_1 a\cos x_4 - bK_4}{M_1(x_1+ex_3)}+\frac{K_2 a\cos x_4 - bK_3}{M_1(x_1-ex_3)}-\Gamma_1\right] \quad (70)$$

$$\Gamma_1=\frac{(am_{uf}-bm_{ur})}{M_1} \quad (71)$$

$$a_{24}=\frac{(K_1+K_2)\cos x_4}{M_1} \quad (72)$$

$$a_{25}=\frac{J_1\sin x_4}{M_1} \quad (73)$$

$$a_{26}=\frac{J_2\sin x_4}{M_1} \quad (74)$$

$$a_{27}=a_{28}=a_{31}=0 \quad (75)$$

$$a_{32}=-\left[\frac{K_1(a\cos x_4 - e\sin x_4)-bK_4}{I_z(x_1+ex_3)}+\Gamma_2\right] \quad (76)$$

$$\Gamma_2=\frac{K_2(a\cos x_4 - e\sin x_4)-bK_3}{I_z(x_1-ex_3)} \quad (77)$$

$$a_{33}=-\left[\frac{K_1 a(a\cos x_4 - e\sin x_4)-b^2K_4}{I_z(x_1+ex_3)}+\Gamma_3\right] \quad (78)$$

$$\Gamma_3=\frac{K_2 a(a\cos x_4 - e\sin x_4)+b^2K_3}{I_z(x_1-ex_3)} \quad (79)$$

$$a_{34}=\frac{K_1(a\cos x_4 - e\sin x_4)+K_2(a\cos x_4 + e\sin x_4)}{I_z} \quad (80)$$

$$a_{35}=\frac{J_1(a\sin x_4 + e\cos x_4)}{I_z} \quad (81)$$

$$a_{36}=\frac{J_1(a\sin x_4 - e\cos x_4)}{I_z} \quad (82)$$

$$a_{37}=-e\frac{J_3}{I_z},\ a_{38}=e\frac{J_4}{I_z} \quad (83)$$

$$a_{41}=a_{42}=a_{43}=a_{45}=a_{46}=a_{47}=a_{48}=0 \quad (84)$$

$$a_{44}=1/\tau \quad (85)$$

For each wheel (i = 5, 6, 7, 8), following coefficients are calculated.

$$a_{i1}=-\frac{R_i^2 J_i x_i}{I_w x_1}-(x_i+1)\frac{A_p|x_1|}{M_1} \quad (86)$$

$$a_{i2}=-\frac{(x_i+1)}{x_1}\left[\frac{K_1\sin x_4}{M_1(x_1+ex_3)}+\frac{K_2\sin x_4}{M_1(x_1-ex_3)}+x_3\right] \quad (87)$$

$$a_{i3}=\frac{(x_i+1)}{x_1}\left[\frac{K_1 a\sin x_4}{M_1(x_1+ex_3)}+\frac{K_2 a\sin x_4}{M_1(x_1-ex_3)}\right] \quad (88)$$

$$a_{i4}=\frac{(x_i+1)}{x_1}\left[(K_1+K_2)\sin x_4\right] \quad (89)$$

$$a_{i5}=-\frac{J_1(x_i+1)\cos x_4}{M_1 x_1} \quad (90)$$

$$a_{i6}=-\frac{J_2(x_i+1)\cos x_4}{M_1 x_1} \quad (91)$$

$$a_{i7}=-\frac{J_3(x_i+1)}{M_1 x_1} \quad (92)$$

$$a_{i8}=-\frac{J_4(x_i+1)}{Mx_1} \quad (93)$$

Similarly, the input matrix B(x) coefficients are calculated in (94-99)

$$b_{12}=\frac{m_s h_s x_3}{M_1} \quad (94)$$

$$b_{21}=\frac{m_s h_s C_\varphi}{I_{xx}M_1} \quad (95)$$

$$b_{22}=\frac{m_s g h_s K_\varphi}{I_{xx}M_1} \quad (96)$$

$$b_{ii}=-\frac{R_i^2 J_i}{I_w x_1} \quad (97)$$

$$b_{i2}=\frac{x_i+1}{M_1 x_1}m_s h_s x_3 \quad (98)$$

$$b_{44}=-\frac{1}{\tau} \quad (99)$$

ACKNOWLEDGMENT

The authors would like to thank Universiti Teknologi Malaysia and the Ministry of Education Malaysia for their support for providing Carsim software and Myvi car.

REFERENCES

[1] J. He, D.A. Crolla, M.C. Levesley and W.J. Manning, "Coordination of active steering, driveline and braking for Integrated vehicle Dynamics," Part D. Journal of Automobile Engineering, no.10, vol. 220, 2006. doi:10.1243/09544070JAUTO265

[2] M. K., Aripin, et al., "A Review of Active Yaw Control System for Vehicle Handling and Stability Enhancement," International Journal of Vehicular Technology, vol. 2014. doi:10.1155/2014/437515.

[3] D. Li, S. Du, and F. Yu, "Integrated vehicle chassis control based on direct yaw moment, active steering and active stabilizer." Vehicle System Dynamics. vol. 46, no. S1, pp. 341-351, 2009. doi:10.1080/00423110801939204.

[4] S. C. Baslamisli, I. E. Kose and G. Anlac, "Handling stability improvement through robust active front steering and active differential control," Vehicle System Dynamics, vol. 49, no. 5, pp. 657-683, 2011. doi:10.1080/00423111003671900.

[5] M. Abe, N. Ohkubo, and Y. Kano, "A direct yaw moment control for improving limit performance of vehicle handling-comparison with 4WS," Vehicle System Dynamics, vol. 25, no. S1, pp. 3-23, 1996. doi:10.1080/00423119608969184.

[6] Y. Furukawa and M. Abe, "Advanced chassis control systems for vehicle handling and active safety," Vehicle System Dynamics. vol. 28, no. 2-3, pp. 59-86, 1997. doi: 10.1080/00423119708969350.

[7] M. Nagai, "The perspective of research for enhancing active safety based on advanced control technology," Vehicle System Dynamics, vol. 45, no. 5, pp. 413-431, 2007. doi:10.1080/00423110701275162.

[8] F. Tahami, S. Farhangi and R. Kazemi, "A Fuzzy Logic Direct Yaw-Moment Control System for All-Wheel-Drive Electric Vehicles," Vehicle System Dynamics, no.41, vol.3, pp. 203-221, 2004. doi:10.1076/vesd.41.3.203.26510.

[9] B. L. Boada, M. J. L. Boada and V. Diaz, "Fuzzy Logic applied to yaw moment control for vehicle stability," Vehicle System Dynamics and Mobility, vol. 43, no. 10, pp. 753-770, 2005. doi:10.1080/00423110500128984.

[10] L. Junwei and Y. Huafang, "Fuzzy logic applied to yaw moment control for vehicle stability," in Mechatronics and Automation, 2009. ICMA2009. International Conference on IEEE 2009. doi:10.1109/icma.2009.5245096.

[11] J. Wang and R. G. Longoria, "Coordinated and Reconfigurable vehicle dynamics control," Control System Technology, IEEE

Transactions. vol. 17, no. 3, pp. 729-732, 2009. doi:10.1109/TCST.2008.2002264.

[12] N. Hamzah, M. K. Aripin, Y. M. Sam, H. Selamat, M. F. Ismail, "Vehicle Stability Enhancement based on second order sliding mode control.," Control System, Computing and Engineering, ICCSCE, 2012 IEEE International Conference pp. 580-585, 2012. doi:10.1109/iccsce.2012.6487212.

[13] E. Ono, S. Hosoe., S. Doi., K. Asano., Y. Hayashi. "Theoratical Approach for improving the vehicle robust stability and maneuverabilityby active front wheel steering control." Vehicle System Dynamics, vol. 29, no. S1, pp. 748-753, 1998. doi:10.1080/00423119808969603.

[14] X. Yang, Z. Wang and W. Peng, "Coordinated Control of AFC and DYC for Vehicle handling and Stability Based on Optimal Guaranteed Cost Theory." Vehicle System Dynamics. vol. 47, no. 1, pp. 57-79, 2009. doi:10.1080/00423110701882264.

[15] X. Shen and F. Yu, "Investigation of Integrated Vehicle Chassis Control based on Vertical and Lateral Tyre behaviour correlativity," Vehicle System Dynamics, vol. 44, pp. 506-519, 2006. doi:10.1080/00423110600875252.

[16] T. Acarman, "Nonlinear optimal integrated vehicle control using individual braking torque and steering angle with online control allocation by using state dependent Riccati equation technique," Vehicle System Dynamics, vol. 47, no. 2, pp. 155-177, 2009. doi:10.1080/00423110801932670.

[17] B. A. Güvenç, T. Acarman and L. Guvenc, "Coordination of steering and individual wheel braking actuated vehicle yaw stability control," Intelligent Vehicle Symposium, 2003 Proceedings. IEEE. pp. 288-293, 2003. doi:10.1109/IVS.2003.1212924.

[18] F. Yu, D. F. Li and D. A. Crolla, "Integrated Vehicle Dynamics control-state-of-the art review", Vehicle Power and Propulsion Conference, 2008 VPPC'08 IEEE, IEEE, pp. 1-6, 2008. doi:10.1109/VPPC.2008.4677809.

[19] W. Cho, J. Yoon, J. Kim, J. Hur and K. Yi, "An investigation into unified chassis control scheme for optimized vehicle stability and manoeuvrability," Vehicle System Dynamics. vol. 46, no. S1, pp. 87-105, 2008. doi:10.1080/00423110701882330.

[20] A. Elmarakbi, C. Rengaraj, A. Wheately and M. Elkady, "New integrated chassis control systems for vehicle handling performance enhancement,"International Journal of Dynamics and Control, vol. 1, no. 4, pp. 360-384, 2013. doi:10.1007/s40435-013-0026-9.

[21] J. S. Yu, "A robust adaptive wheel-slip controller for antilock brake system." Decision & control, 1997, Proceedings of the 36th IEEE Conference on. vol. 3, IEEE, 1997. doi:10.1109/cdc.1997.657714.

[22] J. Tjonnas and T. A. Johansen, "Stabilization of automotive vehicles using active steering and adaptive brake control allocation," Control Systems Technology, IEEE Transactions on. vol. 18, no. 3, pp.545-558, 2010. doi:10.1109/TCST.2009.2023981.

[23] S. Mammar and D. Koenig, "Vehicle Handling Improvement by Active Steering," Vehicle System Dynamics, vol. 38, no. 3, pp. 211-2 42,2002. doi:10.1076/vesd.38.3.211.8288.

[24] C. P. Mracek and J. R. Cloutier, "Control Designs for the nonlinear benchmark problem Via the State dependent Ricatti equation," Int. J. Robust Control, vol. 8, pp. 401-433, 1998. doi:10.1002/(SICI)1099-1239(19980415/30)8:4/5<401::AID-RNC361>3.0.CO;2-U.

[25] F. J. D'Amato and D. E. Viassolo, "Fuzzy control for active suspensions," Mechatronics, vol. 10, no. 8, pp. 897-920, 2000. doi:10.1016/S0957-4158(99)00079-3.

[26] S. H. Zareh, A. Sarrafan, A. F. Jahromi, A. A. Khayat, "Linear quadratic gaussian application and clipped optimal algorithm using semi active vibration of passenger car," Mechatronics (ICM), 2011 IEEE International Conference on. IEEE, 2011. doi:10.1109/icmech.2011.5971268.

[27] P. F. Wu and C. F. Yung, "On the geometric and dynamic structures of the H2 optimal and H? central controllers." Automatica, vol.46, no.11, pp. 1824-1828, 2010. doi:10.1016/j.automatica.2010.06.049

[28] R. E. Precup, M. B. Radac, M. L. Tomescu, E. M. Petriu and S. Preitl, "Stable and convergent iterative feedback tuning of fuzzy controllers for discrete-time SISO systems," Expert Systems with Applications , 2013, vol. 40, no.1, pp.188-199. doi:10.101 6/j.eswa.2012.07.023.

[29] R. R. Yacoub, R. T. Bambang, A. Harsoyo and J. Sarwono, "DSP implementation of combined FIR-functional link neural network for active noise control," International Journal of Artificial Intelligence, vol. 12, no. 1, pp.36-47, 2014.

[30] T. T. Wang, W. F. Xie, G. D. Liu and Y. M. Zhao, "Quasi Min-Max Model Predictive Control for Image Based Visual Servoing with Tensor Product Model Transformation," Asian Journal of Control, vol.17, no. 2, pp.402-416. 2015. doi:10.1002/asjc.871.

[31] Fargham Sandhu, Hazlina Selamat, Yahaya MD Sam, "Linear Quadratic Regulator and Skyhook Application in Semiactive MR Damper Full Car Model," Asian Control Conference (ASCC), 2015 10th Asian IEEE, doi:10.1109/ASCC.2015.7244406.